

# **Decomposition Analysis of Neodymium-Loaded Resin**

**September 2013**

**Prepared by  
R. D. Hunley  
S. L. Voit**

## DOCUMENT AVAILABILITY

Reports produced after January 1, 1996, are generally available free via the U.S. Department of Energy (DOE) Information Bridge.

**Web site** <http://www.osti.gov/bridge>

Reports produced before January 1, 1996, may be purchased by members of the public from the following source.

National Technical Information Service  
5285 Port Royal Road  
Springfield, VA 22161

**Telephone** 703-605-6000 (1-800-553-6847)

**TDD** 703-487-4639

**Fax** 703-605-6900

**E-mail** [info@ntis.gov](mailto:info@ntis.gov)

**Web site** <http://www.ntis.gov/support/ordernowabout.htm>

Reports are available to DOE employees, DOE contractors, Energy Technology Data Exchange (ETDE) representatives, and International Nuclear Information System (INIS) representatives from the following source.

Office of Scientific and Technical Information  
P.O. Box 62

Oak Ridge, TN 37831

**Telephone** 865-576-8401

**Fax** 865-576-5728

**E-mail** [reports@osti.gov](mailto:reports@osti.gov)

**Web site** <http://www.osti.gov/contact.html>

This report was prepared as an account of work sponsored by an agency of the United States Government. Neither the United States Government nor any agency thereof, nor any of their employees, makes any warranty, express or implied, or assumes any legal liability or responsibility for the accuracy, completeness, or usefulness of any information, apparatus, product, or process disclosed, or represents that its use would not infringe privately owned rights. Reference herein to any specific commercial product, process, or service by trade name, trademark, manufacturer, or otherwise, does not necessarily constitute or imply its endorsement, recommendation, or favoring by the United States Government or any agency thereof. The views and opinions of authors expressed herein do not necessarily state or reflect those of the United States Government or any agency thereof.

Nuclear Security and Isotope Technology Division

## DECOMPOSITION ANALYSIS OF NEODYMIUM-LOADED RESIN

Riley Hunley and Stewart Voit

Date Published: September 2013

Prepared by  
OAK RIDGE NATIONAL LABORATORY  
Oak Ridge, Tennessee 37831-6283  
managed by  
UT-BATTELLE, LLC  
for the  
U.S. DEPARTMENT OF ENERGY  
under contract DE-AC05-00OR22725



# CONTENTS

	<b>Page</b>
LIST OF FIGURES .....	v
LIST OF TABLES .....	vii
ACKNOWLEDGMENTS .....	ix
EXECUTIVE SUMMARY .....	ix
1. INTRODUCTION .....	1
2. EQUIPMENT AND FEEDSTOCK.....	2
2.1 RESIN .....	2
2.2 RESIN LOADING MATERIALS .....	2
2.3 DECOMPOSITION MATERIALS.....	4
3. EXPERIMENTAL PROCEDURE .....	5
3.1 RESIN LOADING .....	5
3.2 DECOMPOSTION.....	6
3.2.1 Decomposition Procedures.....	7
3.3 PARTICLE AND THERMAL ANALYSIS PROCEDURES .....	9
4. RESULTS.....	10
4.1 DECOMPOSITION RESULTS .....	10
4.1.1 Data for Comparison to Curium Oxide Production Process .....	10
4.1.2 Time and Gas Dependent Decomposition Data .....	11
4.1.3 Temperature-Dependent Decomposition Data.....	11
4.2 PARTICLE ANALYSIS .....	12
4.3 THERMAL ANALYSIS .....	13
5. DISCUSSION.....	14
6. SUMMARY.....	16
REFERENCES.....	17



## LIST OF FIGURES

<b>Figure</b>	<b>Page</b>
Fig. 1. Resin–metal bond.....	2
Fig. 2. Schematic of the resin loading process .....	3
Fig. 3. Resin loading apparatus .....	3
Fig. 4. Furnace with controller .....	4
Fig. 5. Quartz pipe .....	4
Fig. 6. Alumina boat crucible .....	5
Fig. 7. Ion exchange column loading front.....	6
Fig. 8. Heating conditions for Cm-Am oxide production processes .....	7
Fig. 9. Sample color change .....	11
Fig. 10. XRD data for Sample 6.....	12
Fig. 11. SEM imaging of Sample 1 .....	13
Fig. 12. SEM imaging of Sample 2 .....	13
Fig. 13. SEM imaging of Sample 6 .....	13
Fig. 14. STA data on a Nd-loaded resin sample.....	14



## LIST OF TABLES

<b>Table</b>	<b>Page</b>
Table 1. Samples and their heating parameters for the calcination and sintering steps .....	7
Table 2. Results of Nd-loaded resin using the Cm-Am oxide production process.....	10
Table 3. Results of changing gas type or isothermal hold time during the calcination stage.....	11
Table 4. C and S contents at sintering temperature of 1400°C.....	12



## ACKNOWLEDGMENTS

This research was supported by the Isotope Program, Office of Nuclear Physics of the U.S. Department of Energy. The authors are grateful to Robbie Meisner of the High Temperature Materials Laboratory for her efforts in producing the X-ray diffraction results, and to Steve Owens, Julie Ezold, and Jared Johnson of the Nuclear Security & Isotope Technology Division for their overall help and support.

## EXECUTIVE SUMMARY

In an effort to understand and quantify the carbon and sulfur contents of a curium oxide production process performed in the hot cells at Oak Ridge National Laboratory's Radiochemical Engineering Development Center, a non-radioactive surrogate was used in a similar oxide formation process. Neodymium (Nd), which was chosen as a substitute for curium, was loaded onto a Dowex 50W-X8 resin by use of ion exchange column techniques and then treated under a variety of processing conditions. The surrogate product was analyzed for carbon and sulfur impurities, using inductively coupled plasma-mass spectrometry for sulfur assessment, a LECO combustion furnace/analyzer for carbon quantification, and X-ray diffraction for compound identification. The results indicate that the carbon and sulfur contents in the Nd oxide were similar to current estimations for curium oxide using the reference hot cell process. It was also seen that the major surrogate product of the hot cell process contained sulfur in a Nd oxysulfate ( $\text{Nd}_2\text{O}_2\text{SO}_4$ ) compound. Parametric analysis of the resin decomposition process revealed that increasing the temperature to 1400°C yielded considerably better removal of carbon and sulfur.



## 1. INTRODUCTION

The goal of this work was to investigate the thermal decomposition of neodymium (Nd)-loaded resin, quantify the carbon and sulfur contents in the product, and apply the knowledge gained to improve the preparation of actinide oxide material for use in transmutation targets. The actinide oxide production process was developed as a simple and efficient procedure for manufacturing curium–americium (Cm–Am) oxide in a hot cell and was achieved by using a resin-bead loading and calcination process [1]. Cation exchange resins are used as a viable way to form spherical oxide microspheres suitable for use in the fabrication of transmutation targets irradiated in nuclear reactors. The process of forming curium oxide microspheres for target applications through the use of sulfonic cation exchange resins has been employed at the Radiochemical Engineering Development Center (REDC) for several decades. Strong acid resins, such as Dowex 50W-X8, contain sulfonate groups that are very efficient at binding with cations such as Cm or Nd that have a +3 charge state. The phase and chemical composition of the final product from decomposition of the cation-loaded resin can vary depending on the processing conditions. A parametric study was done on the REDC process that produces Cm–Am oxide in order to identify a decomposition process to minimize the residual carbon and sulfur contents in the oxide product resulting from the decomposition of a cation-loaded resin using Nd as a stand-in for Cm.

The Cm–Am oxide is produced and fabricated into target material at the REDC. This Cm oxide target material is blended with aluminum powder, formed into cermet pellets, and then encapsulated in an aluminum target rod for subsequent irradiation in the High Flux Isotope Reactor (HFIR). After irradiation, the pellets are dissolved and processed chemically to separate and recover heavy actinide elements such as berkelium, californium, einsteinium, and fermium for distribution [1]. In order to optimize production and recovery of the transcurium elements, it is necessary to have as much Cm in the original pellets as allowable. One of the key limitations to the actinide loading of a target pellet is the heat transfer characteristic. Target pellets and target rods need to be maintained below a prescribed temperature during irradiation in the HFIR, thus the thermal conductivity of each pellet needs to meet specified criteria. The maximum amount of curium oxide per target presently allowed is based on a very conservative thermal analysis [2] that ensures the target rod centerline temperature remains below 900°F. To avoid exceeding the heat limits, the concentrations of material in each pellet are specified on a volumetric basis. The distribution of each pellet contains roughly 20 vol % void space, 67.7–71.5 vol % aluminum powder, and 8.5–12.3 vol % actinide oxide [3]. The pellet void volume is intended to accommodate gaseous fission products that are generated during irradiation. The chemical “purity” of the actinide oxide is calculated from radiochemical analysis; calorimetric measurement of decay heat; and the assumed oxide stoichiometries  $\text{CmO}_{1.71}$ ,  $\text{AmO}_2$ , and  $\text{PuO}_2$ . The volume of actinide oxide allowed in a pellet includes impurities, which are typically on the order of 10 wt % of the oxide material [1]. These impurities are conservatively assumed to be equal parts elemental carbon and sulfur. Due to the mass of elemental carbon and sulfur compared to Cm, the 10 wt % translates to a relatively high volume percentage of carbon and sulfur in the oxide material, which substantially reduces the total actinide content in each target. Any reduction in the volume of impurities increases the potential amount of actinide per pellet. Increasing the amount of Cm–Am in each pellet decreases the total number of target rods needed to achieve the desired amount of heavy-actinide elements produced, reducing the expenses throughout target production and irradiation.

Special consideration was given to the changes that could be made to the parameters of the Cm–Am oxide microspheres production process. The hot cell process equipment is remotely operated by personnel using mechanical arms (manipulators) that extend through the cell wall, which is 54 in. thick. Major alterations to the established remotely operated process infrastructure could have significant cost and schedule implications; therefore, the existing Cm–Am oxide production process was closely followed during surrogate testing, changing only the practically variable oxide production parameters such as temperature, atmosphere, and heating duration to assess removal of carbon and sulfur.

In this parametric study, a non-radioactive trivalent surrogate was used in place of Cm since a direct use of Cm inside the hot cell is costly and its use in sufficient quantities outside the hot cells is not possible due to its highly radioactive nature. Neodymium was chosen for this study as it is the historical surrogate of choice for americium [4, 5, 6] and the common surrogate for curium in other research [7, 8, 9], and because of the relative ease of analyzing Nd. Consideration was given to using additional rare earth surrogates, but it was determined that any additional data collected would not be within the scope of this research.

## 2. EQUIPMENT AND FEEDSTOCK

### 2.1 RESIN

A Dowex® 50W-X8 cation exchange resin was used with a resin bead diameter of 50–70  $\mu\text{m}$ . The polymer-based beads of the resin contain sulfonic functional groups ( $\text{SO}_4^-$ ) that have a net charge of -1; therefore, it takes three of these functional groups for cations like Cm or Nd to attach to the resin matrix as represented in Fig. 1. The resin was prepared by washing it twice with deionized water, then conditioning it once with 8 M  $\text{HNO}_3$  and then rinsing once more with deionized water. This helped remove some contaminants that were not part of the resin beads (e.g., trace metals) and condition the resin for loading.

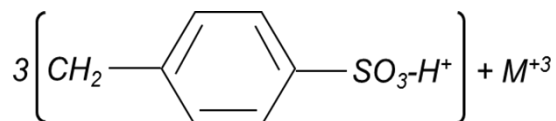


**Fig. 1. Resin–metal bond.** Depiction of the bond between the Nd ( $\text{M}^{+3}$ ) and the sulfonic acid group of the Dowex resin.

### 2.2 RESIN LOADING MATERIALS

A total of about 120 mL of resin was packed in a burette column, and then a small amount of glass wool was put on top of the resin bed to minimize the chance that liquid turbulence would disturb the bed of particles. The column had an approximate inside diameter of 25 mm and a height of about 480 mm above the glass frit. Below the frit was a valve with a drip spout that was attached to a hose. The hose was used to pump the raffinate fluid to a 1000 mL collection container. A Master Flex Easy Load pump with a Master Flex speed controller was used to pump the Nd solution out of the column. Figure 2 depicts the system schematic, and Fig. 3 is a photograph of the actual system used.

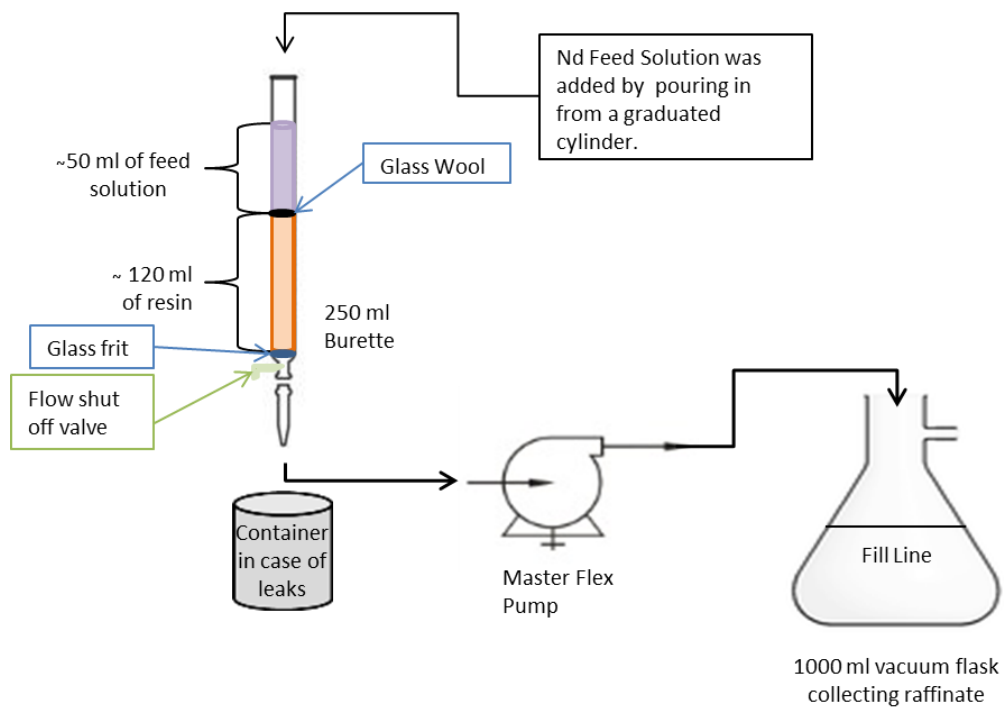


**Fig. 2. Schematic of the resin loading process.**

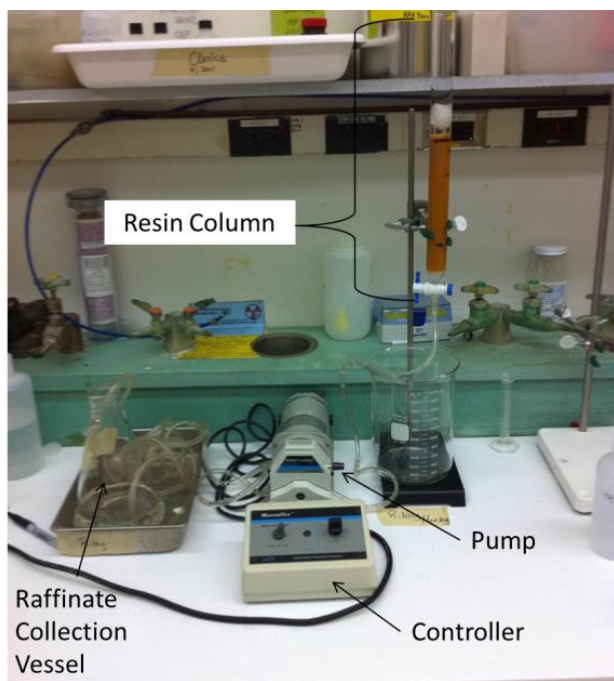


**Fig. 3. Resin loading apparatus.**

### 2.3 DECOMPOSITION MATERIALS

Since the drying and decomposition process was performed by heating the resin in the presence of a flowing gas at 0.3 L/min., equipment had to be selected that would allow for heating in this manner. The main part of the heating element included a Harrop Industries Inc. cylindrical furnace (oriented horizontally) and controller (Fig. 4). For the first two steps within the process, drying and calcination, two custom-made quartz pipes (Fig. 5) were made to go in the openings at each end of the furnace. The pipes had a long narrow stem that allowed for the quartz tubes to be placed inside the heating mantle and for the gas lines to be attached outside the furnace, minimizing the heat on the gas lines. The tube holding the resin was approximately 19 mm in diameter and about 28 mm in height. A quartz frit was placed at the bottom of the tube section to allow the purge gas to flow up through the bed of resin particles. In addition to the furnace and pipes, other items were needed, such as a rotometer to control the gas flow, a vacuum system to remove water from the loaded resin, and glass wool to place over the resin in the tube to minimize blowout during the gas purges. For the sintering steps or any additional heating above 800°C, a ceramic crucible was used (Fig. 6). This was a rectangular alumina crucible approximately 5 cm wide, 7.5 cm long, and 0.64 cm tall. Samples placed in the crucible were spread thin in order to maximize the surface area in contact with the static air to promote oxidation. The same equipment and materials were used for all samples that would be produced.



Fig. 4. Furnace with controller.

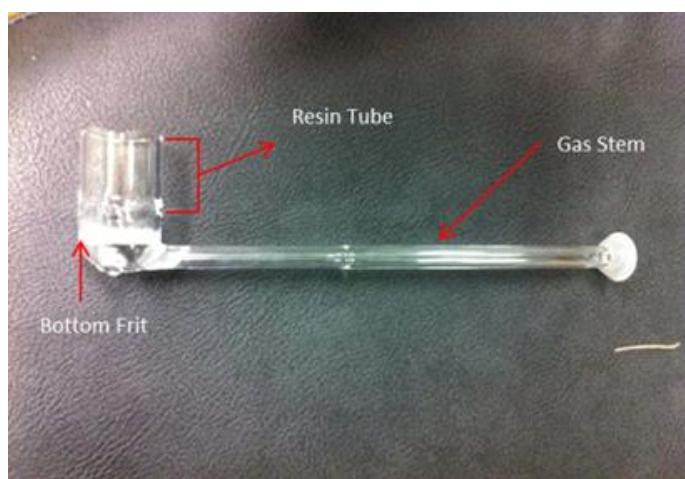


Fig. 5. Quartz pipe.



**Fig. 6. Alumina boat crucible.**

### **3. EXPERIMENTAL PROCEDURE**

#### **3.1 RESIN LOADING**

The resin loading process consists of the following steps: a) equilibration of the resin, b) preparation of the resin column, c) loading of the resin with the Nd feed solution, and d) rinsing with deionized water. The conditioned resin was batch equilibrated to the desired pH by rinsing it with 3 times the volume of the resin bed with a 0.25 M HNO<sub>3</sub> solution. Next, the equilibrated resin was poured into the column 20–25 mL at a time to avoid segregating the particles according to size. The larger particles will settle out first; therefore, a more uniform and reproducible resin column was constructed by pouring the resin in sections [10]. Once all of the resin was in the burette tube and it had settled, the feed solution was poured into the top of the column 50 mL at a time and allowed to collect above the resin bed as the pump on the other end pulled the solution through the resin. A total of about 2000 mL of feed solution was pulled through the column by the pump at a rate of about 3.5 mL min<sup>-1</sup> cm<sup>-2</sup>. The actinide concentration used in the feed solution of the Cm-Am oxide resin loading procedure was 10 g/L [1], meaning the same molarity was achieved by a Nd concentration of about 5.5 g/L. With this information the feed solution was made from 33.418 g of solid neodymium nitrate hexa-hydrate [Nd(NO<sub>3</sub>)<sub>3</sub>•6H<sub>2</sub>O] mixed with 1 L of deionized water and 1 L of 0.5 M HNO<sub>3</sub>. This gave a 0.4 M Nd(NO<sub>3</sub>)<sub>3</sub> in 0.25 M HNO<sub>3</sub> solution for the feed. Surplus feed solution was used to ensure the resin was loaded to excess. As the neodymium solution was being pumped through the resin, a distinct line of color change could be observed, as seen in Fig. 7. This was the loading front of the neodymium. A concentration profile develops as the ion exchange takes place in the resin bed. As the front moves down through the bed, the resin above the front is in equilibrium with the feed solution. The resin below the front is in equilibrium with the previous solution used to equilibrate the resin. Breakthrough of the feed solution occurs when the front reaches the end of the bed. As seen in Fig. 7, the front can be irregular; therefore, breakthrough can occur at one point of the bed and not at another. Continued loading of the feed solution can eventually achieve complete breakthrough, thus the reason for using an excess of the neodymium solution. After the loading of the feed solution, the loaded resin bed was given a deionized water rinse of about 3 times the resin bed volume and stored with deionized water in a bottle until it could be used in the decomposition procedures. Since Nd does not degrade the resin as the decay of Cm and Am does, the Nd-loaded resin can be stored for later use, unlike the Cm-Am-loaded resin, which is subsequently decomposed.



**Fig. 7. Ion exchange column loading front.** The resin in the column is a darker shade on the top portion that was loaded with neodymium, and lighter on the bottom portion, which had not yet been loaded.

### 3.2 DECOMPOSITION

Three main stages are anticipated in the formation of oxide microspheres from the 50W-X8 resin: (1) drying, (2) calcination, and (3) sintering. The drying step was done in exactly the same manner for every sample; any remaining water was removed from the loaded resin before any decomposition began. Drying helped provide more uniform gas flow and kept the resin from lifting out of the tube during subsequent steps. With the assistance of purge gases, the majority of the decomposition took place in the calcination step, which consisted of a burning segment where the hydrocarbon chain decomposes, a sulfur removal segment that was assisted by a change in purge gas, and then an oxidation period [1,7]. These transitions are not precise and depend upon the heating conditions. After the calcination stage, the sintering step was initiated. It entailed heating the sample to high temperatures and allowing the small particles to continue oxidation.

In an effort to obtain a base comparison to the Cm-Am oxide production process, a Nd oxide sample was produced that followed the heating procedures of the REDC Cm-Am oxide production process. The general decomposition procedure of the Cm-Am-loaded resin is depicted in Fig. 8. These same procedures were used for Sample 1 to permit a direct comparison and are detailed in Section 3.2.1.1. Eight other samples were prepared by the same basic procedures as for the first sample. The results from these samples were used to understand the differences in sulfur and carbon residues from the original hot cell process when the temperature, time heated, or gas purge sequence was altered. It was thought one of these alterations could possibly enhance the understanding of the production pathway for the oxide.

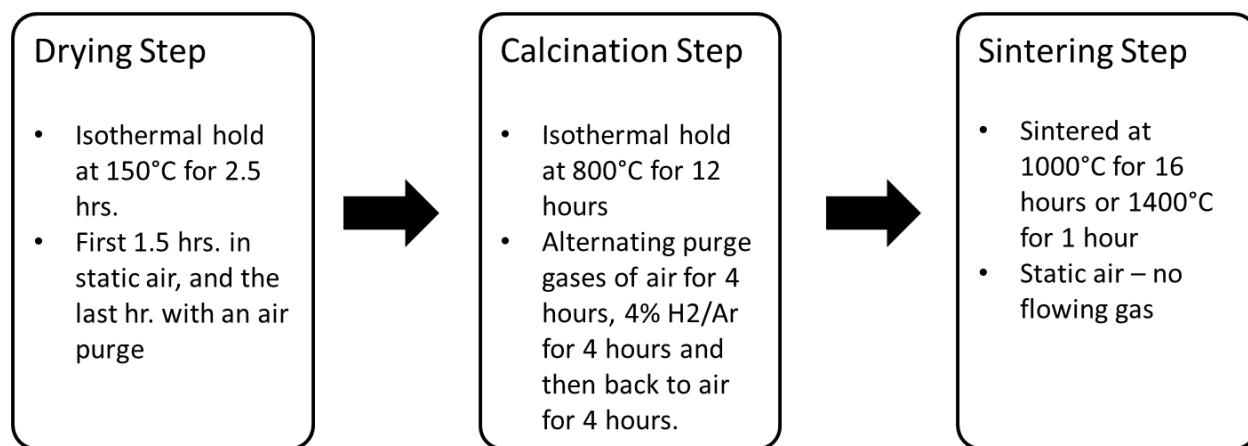


**Fig. 8. Heating conditions for Cm-Am oxide production processes.**

### 3.2.1 Decomposition Procedures

Samples were prepared by pouring a resin-deionized water slurry resin into the tube section of the pipes (Fig. 5), and any excess water was pumped out using a vacuum pump and flask. This left a resin bed in the tube above the glass frit. The gas purge lines were connected to the pipes, and they were placed in each end of the Harrop Industries Inc. round furnace. Next, the drying stage was executed by heating the resin at 5°C/min to 150°C and holding it at 150°C for 2.5 hours, for a total of 3 hours of drying. The first two hours were in static air, and the last hour had a gas purge of air. The pipes were then cooled and the weight of each measured so that the amount of mass lost from each step could be calculated going forward. The calcination and sintering steps were different for each of the nine samples, and the procedures for each are discussed in detail below. Table 1 lists the samples and heating parameters for

**Table 1. Samples and their heating parameters for the calcination and sintering steps**

Sample No.	Purpose of Sample	Heating Parameters
1	Base case to compare with the Cm oxide process	Decompose at 800°C for 12 h total using alternating purge gases of air for 4 h, 4% H <sub>2</sub> /Ar for 4 h, and back to air for 4 h; then sinter the sample at 1000°C for 16 h in static air
2	Initial decomposition of the base case	Decompose at 800°C for 12 h total using alternating purge gases of air for 4 h, 4% H <sub>2</sub> /Ar for 4 h, and back to air for 4 h
3	Gas purge of air only	Decompose at 800°C for 8 h using a purge gas of air
4	Gas purge for sulfur removal	Decompose at 800°C for 4 h using a purge gas of 4% H <sub>2</sub> /Ar
5	Gas sequence changed during decomposition	Decompose at 800°C for 12 h total using purge gases of 4% H <sub>2</sub> /Ar for 4 h and air for 8 h
6	Increase sintering temperature of the base case	Decompose identical to sample 2; then sinter the sample at 1400°C for 1 h in static air
7	Increase the temperature of sample 3	Decompose at 800°C for 8 h using a purge gas of air; then sinter the sample at 1400°C for 1 h in static air
8	Increase the temperature of sample 4	Decompose at 800°C for 4 h using a purge gas of 4% H <sub>2</sub> /Ar; then sinter the sample at 1400°C for 1 h in static air
9	Increase the temperature of sample 5	Decompose at 800°C for 12 h total using purge gases of 4% H <sub>2</sub> /Ar for 4 h and air for 8 h; then sinter the sample at 1400°C for 1 h in static air

each. After the desired heating, each sample was collected and sent to Materials and Chemicals Lab Inc. for sulfur and carbon quantification. Small parts of each sample were also sent to the High Temperature Materials Laboratory for X-Ray Diffraction (XRD) analysis.

### **3.2.1.1 Sample 1**

In order to assess and compare the carbon and sulfur contents of the Nd oxide to the current Cm-Am oxide produced in the hot cell, Sample 1 was made by following exactly the same heating schedule used to produce Cm-Am oxide. After the drying step, the burning step was achieved by heating the resin to 800°C over a 2 hour period and then holding it at 800°C for 2 more hours, all with an air purge. The segment to remove sulfur while preventing further oxidation was done by holding the sample at 800°C and switching the gas purge from air to 4% H<sub>2</sub>/Ar gas for 4 hours. Next, the oxidation step was initiated by continuing to hold the temperature at 800°C and switching the gas purge back to air for 4 more hours. After the sample was cooled and the mass was taken, the oxide was transferred to a crucible to be put back in the furnace for the sintering step. In the sintering phase, the oxide is exposed to static air inside the furnace (no forced air flow), heated to 1000°C at 7°C/min., and held at 1000°C for 16 hours. The sample prepared under these conditions should be representative of the Cm-Am oxide produced in the hot cell.

### **3.2.1.2 Sample 2**

To understand the carbon and sulfur that remained in the calcination product before sintering is done during the hot cell process, the second sample consisted of just the drying and calcination steps. These steps were identical to Sample 1 at 800°C. After the drying step, the resin was heated to 800°C over a 2 hour period and then held at 800°C for 2 more hours, all with an air purge. The sulfur removal segment was initiated by holding the sample at 800°C and switching the gas purge from air to 4% H<sub>2</sub>/Ar gas for 4 hours. Lastly, the temperature was held at 800°C and the gas purge was switched back to air for 4 more hours. At the end of this schedule, the furnace was cooled and the final mass of the sample was determined.

### **3.2.1.3 Sample 3**

To test for the possibility that using 4% H<sub>2</sub>/Ar gas for sulfur removal during the hot cell process was unnecessary, Sample 3 used only a flow gas of air and was heated for 8 hours. The first 2 hours were a ramp up to 800°C, and the last 6 hours were an isothermal hold at that temperature. If enough removal of carbon and sulfur were to occur without using the 4 % H<sub>2</sub>/Ar gas, then the process could be looked at further to optimize the gas sequence and time parameters by eliminating that step. Sample 3 was also used to give a partial examination of the last 8 hours of Sample 5 at 800°C.

### **3.2.1.4 Sample 4**

For Sample 4, the Nd-loaded resin was heated with a flowing gas of 4% H<sub>2</sub>/Ar. The ramp up to 800°C occurred during the first 2 hours, and the last 2 hours consisted of an isothermal hold at 800°C. This sample was produced to evaluate the sulfur removal process from the loaded resin before any decomposition could be accomplished. It gave insight into the removal of sulfur with H<sub>2</sub> gas. Also, it provided some additional comparisons, since it was identical to the first 4 hours of Sample 5.

### **3.2.1.5 Sample 5**

In an effort to understand how the gas purge sequence effected the calcination of the loaded resin, the

order of the purge gases during the calcination step was switched. Specifically, after the drying step, the sample was heated to 800°C over a 2 hour period and held at 800°C for 2 more hours. All 4 hours of this segment had a gas purge of 4% H<sub>2</sub>/Ar. Then 8 hours of air purge was done at 800°C to complete the 12 hour calcination stage. In comparison to the hot cell process, the sulfur removal period of this sample was forced to begin first instead of the burning period by switching the purge gas during the first 4 hours of heating from air to 4% H<sub>2</sub>/Ar. This was considered to be beneficial, as the sulfur might be removed before becoming entrained within the microspheres as the resin decomposed.

#### **3.2.1.6 Sample 6**

To measure the impact of temperature on the Cm-Am oxide production procedure, another sample was produced using the same heating conditions as Sample 2 for the calcination step, but it was then heated further to 1400°C at 8°C/min. in static air and held there for 1 hour. The 1400°C heating temperature used was based on the findings by Hale and Voit [5,7] that suggested the most complete conversion to the oxide took place between 1200 and 1350°C or beyond. For Samples 6 through 9, the 1400°C temperature was used to understand the impact that increasing the sintering temperature had on the oxide content compared to the gas sequence.

#### **3.2.1.7 Sample 7**

The temperature variable was also tested on a sample that had the same heating conditions at 800°C as Sample 3. It was ramped to 800°C over a 2 hour period and held at 800°C for 6 more hours, all with a purge gas of air for a total of 8 hours. But once the material completed the heating at 800°C, it was cooled, weighed, and then placed in an alumina crucible and ramped to 1400°C at a rate of 8°C/min in static air. An isothermal hold at 1400°C for 1 hour completed the decomposition schedule, and afterward the sample was cooled, weighed, and collected for analysis. This sample provided a comparison for the amount of sulfur and carbon that could be removed with an increase in temperature.

#### **3.2.1.8 Sample 8**

Sample 8 tested the influence of increasing the temperature when sintering a sample treated identical to Sample 4 in the calcination step. After heating the sample to 800°C over a 2 hour period with a 4% H<sub>2</sub>/Ar gas purge and an isothermal hold for 2 more hours, the sample was cooled and weighed. It was put into an alumina crucible and then inserted into the furnace where the temperature was increased to 1400°C with a ramp of 8°C/min. Once at the desired temperature, the sample was held there for 1 hour, then cooled, weighed, and collected. The heating at 1400°C was done in static air.

#### **3.2.1.9 Sample 9**

By use of the same conditions at 800°C for Sample 5 and then increasing the temperature, the impact of temperature increase on carbon and sulfur removal, compared to changing the gas sequence, could be seen. After Sample 9 had been heated exactly the same as Sample 5, it was cooled, weighed, and placed in an alumina crucible for sintering at 1400°C. The sample was then ramped to 1400°C at 8°C/min in static air and afterward held at 1400°C for 1 hour.

### **3.3 PARTICLE AND THERMAL ANALYSIS PROCEDURES**

Further understanding of the oxide material and its production pathway was gained by performing additional testing. The Nd-loaded Dowex® resin was analyzed by Differential Scanning Calorimetry/Thermal Gravimetric Analysis (DSC/TGA) and data was gathered using a Simultaneous Thermal Analyzer (STA) 1500 instrument at the High Temperature Material Laboratory in a flowing air

atmosphere on a ramp of 5°C/min up to 1400°C. The DSC/TGA plot produced was used to gather initial understanding for the thermal processes that might be taking place during decomposition. Scanning electron microscopy (SEM) was performed by Materials and Chemicals Lab, Inc. to analyze the characteristic shape and geometry of the calcined microspherical particles.

## 4. RESULTS

Carbon analysis was performed with a LECO combustion furnace/analyzer. ICP-MS was used to find the amount of sulfur in each sample. XRD data was obtained by performing scans on the Panalytical Xpert diffractometer using MoK $\alpha$  radiation, and then a search match was conducted with Jade and/or Highscore software and the ICDD database. The XRD data allowed the sample compounds and phases to be identified, as well as the quantity of each compound contained in the sample.

### 4.1 DECOMPOSITION RESULTS

#### 4.1.1 Data for Comparison to Curium Oxide Production Process

Table 2 shows the weight percentage of carbon and sulfur in the products as well as the Nd compound makeup. These samples are used for direct comparison to the Cm-Am oxide produced. The table also indicates the temperature at which the sample was heated, the length of time it was heated, and the atmosphere.

**Table 2. Results of Nd-loaded resin using the Cm-Am oxide production process**

Sample	Temp (°C)	Time Heated (hr)	Atmosphere	Wt.%		% Nd <sub>2</sub> O <sub>2</sub> S	% Nd <sub>2</sub> O <sub>2</sub> SO <sub>4</sub>	% Nd <sub>2</sub> O <sub>3</sub>
				Carbon	Sulfur			
1	1000	16	Static Air	0.072	6.835	0	86.9	13.1
2	800	12	Flowing Air & H <sub>2</sub> /Ar	0.1375	6.805	0	82.6	17.4
6	1400	1	Static Air	0.086	0.124	0	0	100

Sample 1 was produced to provide results of a surrogate process comparable to the REDC decomposition process. The Nd sample produced contained sulfur at much higher levels than carbon with 6.835 wt % sulfur and 0.072 wt % carbon (Table 2). This sample was found to be mostly Nd<sub>2</sub>O<sub>2</sub>SO<sub>4</sub> (86.9%), with only 13.1% Nd<sub>2</sub>O<sub>3</sub>. Sample 2 was the neodymium compound prepared with only the 800°C hot cell processing steps, and it was not significantly different from Sample 1 in the amounts of sulfur and carbon. Sample 2 contained 6.805 wt % sulfur and only 0.1375 wt % carbon and was found to be 82.6% Nd<sub>2</sub>O<sub>2</sub>SO<sub>4</sub> and 17.4% Nd<sub>2</sub>O<sub>3</sub>. As seen in Fig. 9, the color of the sample was a very light blue, and as with Sample 1 that was heated at a temperature of 1000°C, it could be seen as a mixture of light blue and white particles. Sample 6 was prepared to evaluate the impact that an increase in sintering temperature from 1000°C to 1400°C would have on the amount of carbon and sulfur contaminants and the amount of oxide produced after using the 800°C hot cell processing steps. The sample contained much less sulfur (0.124 wt %) than the samples heated at lower temperatures, and the carbon content remained about the same (0.086 wt %). However, at the 1400°C temperature, Sample 6 was found to be completely converted to the oxide form. In fluorescent lighting Sample 6 (heated at 1400°C) was seen to be blue in color, whereas Samples 1 and 2 (heated at lower temperatures) were both very pale blue. Visual observation in Fig. 9 agrees with other documentation that states the pale blue color is associated with an oxysulfate, while the deeper blue color is identified as an oxide [7].



**Fig. 9. Sample Color Change.** The color changes with increasing temperature from left to right. Far left is Sample 1, middle is Sample 2, and on the right is Sample 6.

#### 4.1.2 Time and Gas Dependent Decomposition Data

To assess the current calcination procedures used in the REDC process, the isothermal hold time and gas purge sequence was varied, and the dependency of the formation of  $\text{Nd}_2\text{O}_3$  based on those two variables was studied at  $800^\circ\text{C}$  (Table 3). Samples 2 and 5 produced using the full 12 hour calcination step had sulfur contents of 6.805 and 7.87 wt %, respectively. Samples 3 and 4 had sulfur contents of 9.925 and 10.295 wt % (Table 3), respectively, when the different gas purge sections were split. The weight percentage of carbon was quite low ( $<0.25\%$ ) when the sample was heated with an air purge. However, Sample 4, which used only 4%  $\text{H}_2/\text{Ar}$  for 4 hours, had a high amount of carbon (roughly 45 wt %) since its gas type hindered oxidation decomposition. Samples 2, 3, and 5 had a high phase fraction of  $\text{Nd}_2\text{O}_2\text{SO}_4$  (82–91%), with the remaining fraction of Samples 3 and 5 being a neodymium oxysulfide compound ( $\text{Nd}_2\text{O}_2\text{S}$ ). Although conversion to the oxide was not complete by the end of any heating at  $800^\circ\text{C}$ , it was found through XRD that only Sample 2 contained any  $\text{Nd}_2\text{O}_3$ . Processing conditions for Sample 2 were the same as the conditions used in the hot cell at the REDC for the Cm-Am oxide process up to  $800^\circ\text{C}$ .

**Table 3. Results of changing gas type or isothermal hold time during the calcination stage**

Sample	Temp. ( $^\circ\text{C}$ )	Time Heated (hr)	Atmosphere	Wt.%		% $\text{Nd}_2\text{O}_2\text{S}$	% $\text{Nd}_2\text{O}_2\text{SO}_4$	% $\text{Nd}_2\text{O}_3$
				Carbon	Sulfur			
2	800	12	4 hr. Air, 4 hr. 4% $\text{H}_2/\text{Ar}$ , 4 hr. air	0.1375	6.805	0	82.6	13.4
3	800	8	Air	0.2255	10.295	27.2	72.8	0
4	800	4	4% $\text{H}_2/\text{Ar}$	45.065	9.925	N/A <sup>a</sup>	N/A <sup>a</sup>	N/A <sup>a</sup>
5	800	12	4 hrs. 4% $\text{H}_2/\text{Ar}$ , then 8 hrs. Air	0.075	7.87	8.9	91.1	0

<sup>a</sup> Sample contained too much organic structure to be identified using XRD.

#### 4.1.3 Temperature-Dependent Decomposition Data

The samples produced at  $800^\circ\text{C}$  by varying the time and gas purge (2, 3, 4, 5) were heated to  $1400^\circ\text{C}$  in order to see the effects of higher temperature on reducing the carbon and sulfur in the oxide material. All samples heated to the higher temperature presented amounts of carbon similar to those of the  $800^\circ\text{C}$  and

1000°C samples but with substantially lower levels of sulfur (Table 4). Heating to 1400°C produced complete conversion to Nd<sub>2</sub>O<sub>3</sub> according to XRD analysis, such as in Fig. 10, along with trace impurities of carbon and sulfur. However, it was seen that replicated samples heated to 1400°C showed varied amounts of neodymium hydroxide [Nd(OH)<sub>3</sub>] along with the sesquioxide; the presence of the hydroxide is discussed later in Section 5.

**Table 4. C and S contents at sintering temperature of 1400°C**

Sample	Temp. (°C)	Time Heated (hr)	Atmosphere	Wt. %		% Nd <sub>2</sub> O <sub>2</sub> S	% Nd <sub>2</sub> O <sub>2</sub> SO <sub>4</sub>	% Nd <sub>2</sub> O <sub>3</sub>
				Carbon	Sulfur			
6	1400	1	Static Air	0.086	0.124	0	0	100
7	1400	1	Static Air	0.0635	0.4165	0	0	100
8	1400	1	Static Air	0.0485	0.2015	0	0	100
9	1400	1	Static Air	0.1325	0.1212	0	0	100

Note: All samples in this table were heated at 1400°C for 1 hour after a 7°C/min ramp in static air.

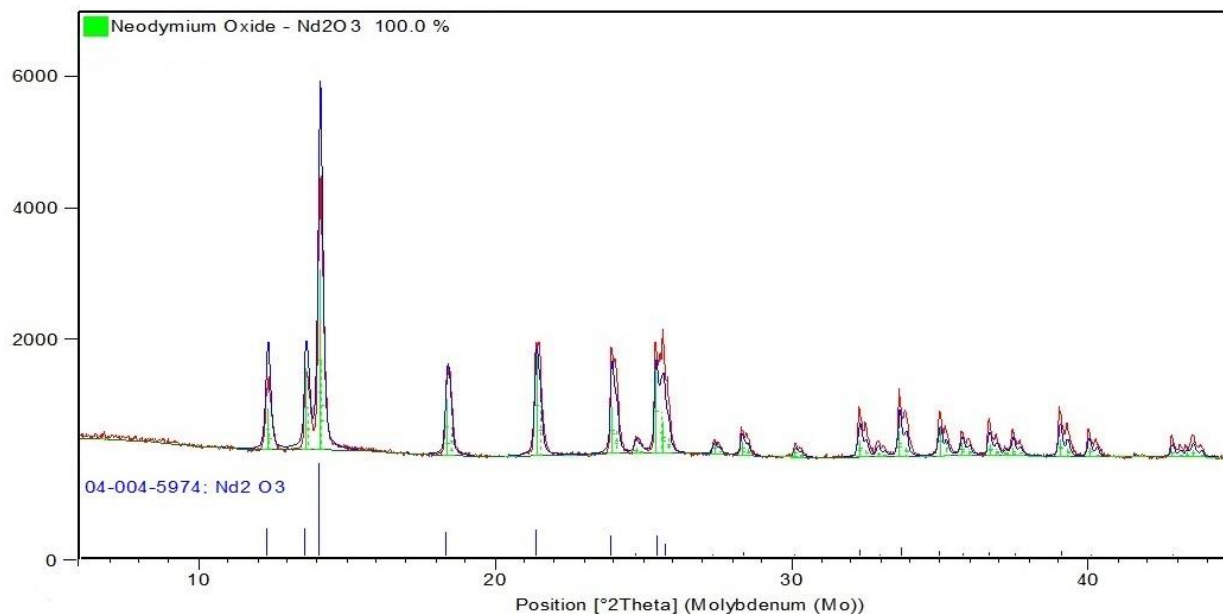


**Fig. 10. XRD data for Sample 6.**

## 4.2 PARTICLE ANALYSIS

The size and shape of microspherical particles that make up the oxide can be important to the appropriate formation of the target pellets. Therefore, the particles in the powders formed from heating the Nd-loaded resin were analyzed at three different temperatures using SEM, and the images are shown in Figs. 11 through 13. Samples prepared identically to those listed in Table 2 (Samples 1, 2, and 6) were analyzed to determine the particle size and geometry after a particular heating sequence. It was observed that as the temperature increased, more fragmentation of the microspheres occurred. At 800°C, the diameter of the spheres averaged about 22–24 μm with a total average particle diameter (including fragments) of 10.85 μm. The particles at 1000°C were mostly fragments that varied widely in size, with the overall average diameter being 9.97 μm and the average sphere diameter being 24–26 μm. At 1400°C, the

compositions of most all the particles were groups of fragments similar to that of Fig. 13, with an overall average diameter of 4.28  $\mu\text{m}$ . No conclusive evidence of any permanent agglomeration of the smaller fragments was seen.

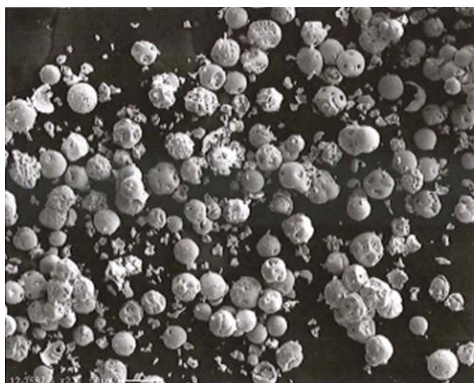


**Fig. 11. SEM imaging of Sample 1.**

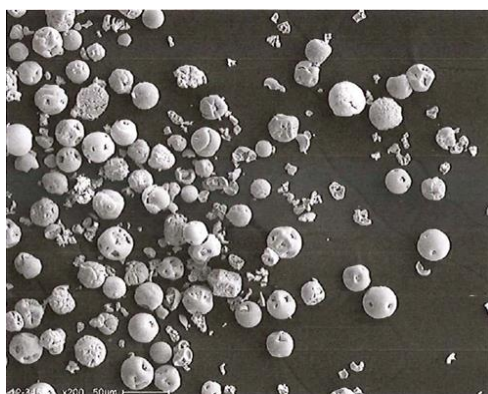


**Fig. 12. SEM imaging of Sample 2.**

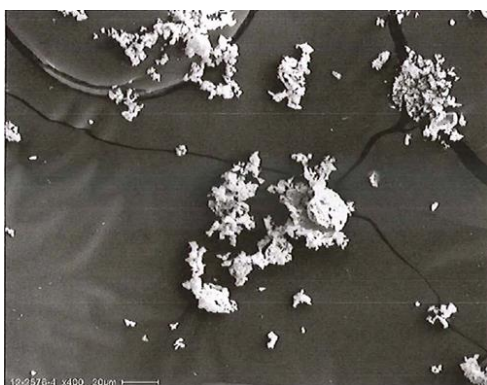


**Fig. 13. SEM imaging of Sample 6.**

#### **4.3 THERMAL ANALYSIS**

To assess the thermal changes during the decomposition process, STA data was collected on a sample of Dowex® resin loaded with Nd. The DSC/TGA plot shown in Fig. 14 was used as an initial benchmark for

information on the decompositions taking place. Several variables in Fig. 14 were tracked over time. The temperature change was held at a constant rate and is shown by the red linearly increasing line. The black curve shows the weight change, the green curve displays the temperature difference between the sample and the heating element, and the blue curve is the derivative of the weight change (i.e., degree of change in weight). Two major mass loss steps appeared on the black line. The first starts at about 100°C and lasts until about 200°C. The second occurs from about 400°C and continues until about 1000°C. One final mass loss can be seen at about 1200°C along with a rise in the derivative of the weight change. A slight exothermic rise can also be seen at this point.

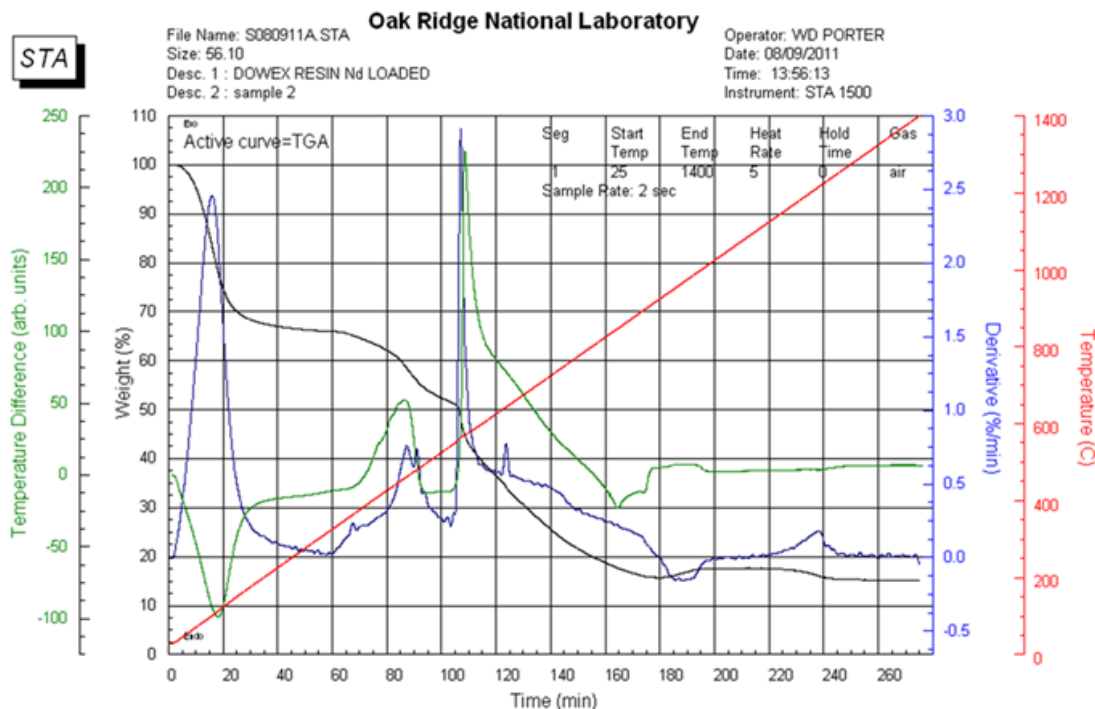


Fig. 14. STA data on a Nd-loaded resin sample.

## 5. DISCUSSION

The three main compounds identified through XRD after decomposing the Nd-loaded resin were the hexagonal structured neodymium oxysulfide ( $\text{Nd}_2\text{O}_2\text{S}$ ), a monoclinic neodymium oxysulfate ( $\text{Nd}_2\text{O}_2\text{SO}_4$ ), and a hexagonal oxide ( $\text{Nd}_2\text{O}_3$ ). The sequence of the compound transition as the resin matrix was being decomposed could provide indication on the level of oxidation of the product. The Dowex® resin utilizes sulfonic acid groups within the resin as mentioned in Section 2.1. The loading process exploits the sulfonic group to attach the cation to it or, in this case, a Nd cation as seen in Fig. 1. Research suggests that after an initial destruction of the resin matrix [7], a reduction of the Nd sulfate complex within the resin would reduce to the oxysulfide ( $\text{Nd}_2\text{O}_2\text{S}$ ) [7, 11]. From that point other research suggests that oxidation of the oxysulfide compound ( $\text{Nd}_2\text{O}_2\text{S}$ ) gives the oxysulfate ( $\text{Nd}_2\text{O}_2\text{SO}_4$ ), and even further oxidation at higher temperatures produces the oxide [7, 12]. Although there could easily be different thermodynamic pathways, the products achieved through the processing conditions used in this research seem to follow the described pattern. It follows a trend that a resin sulfate matrix is decomposed in air and reduced to the oxysulfide ( $\text{Nd}_2\text{O}_2\text{S}$ ) using a  $\text{H}_2/\text{Ar}$  gas, which is then oxidized in air to the oxysulfate ( $\text{Nd}_2\text{O}_2\text{SO}_4$ ) and then further oxidized into the oxide ( $\text{Nd}_2\text{O}_3$ ) [13]. It has been shown that in similar atmospheres, curium has comparable decomposition intermediates [14].

The decomposition process and the results of this research were anticipated from documentation [1, 4, 7] and from the DGA/TGA results shown in Fig. 14. The plot shows some significant features about the formation temperatures of the product of the Nd-loaded resin. The first was an endothermic reaction due to the removal of water from the system that occurs from about 100°C and lasts until about 200°C. The second is the main decomposition step that is highly exothermic, in which the hydrocarbon chain decomposes and the Nd metal converts to an oxygen-containing compound (e.g., oxysulfide or oxysulfate). This begins to occur at about 400°C and continues until the mass becomes relatively constant at about 1000°C. At about 1200°C, there was an additional mass loss step and an associated exothermic event. Prior research found that calcination at or above 1200°C, with the heating parameters matching the parameters used in the DSC/TGA in Fig. 14, gave Nd<sub>2</sub>O<sub>3</sub> [7] from its precursor Nd<sub>2</sub>O<sub>2</sub>SO<sub>4</sub>, which was formed mostly from the second major decomposition step.

While the results from the DSC/TGA are helpful, the heating parameters it uses (5°C/min ramp to 1400°C in flowing air) are different from those used in the hot cell. Therefore, the decomposition model described in Section 3.2 was used to provide results comparable to the process taking place in the hot cell. The results shown in Tables 2 and 3 revealed that sulfur is the main element of impurity if the sample is heated at 800°C or 1000°C. Only trace amounts of carbon were seen in any sample that had been heated in air and had gone through the major decomposition of the resin matrix. This result is quite different from the original research using this procedure with Cm [1], which inferred the impurity level of carbon as being typically between 5 and 12%. The XRD results of the Nd samples at 800°C and 1000°C matched patterns corresponding to an oxysulfate (Nd<sub>2</sub>O<sub>2</sub>SO<sub>4</sub>) as the dominant compound in the product material. Although the oxysulfate was the principal phase present, a small amount of oxide formed in the hot cell process. Because oxide did not form with any other sample at 800°C, the formation of the oxide is attributed to the gas purge sequence. By purging with a hydrogen gas, after an initial oxidation stage, the compound was likely able to be reduced [15], thereby removing more sulfur through H<sub>2</sub>S gas. This allowed the final 4 hours in air at 800°C to fully oxidize more of the sample than if the reduction step using hydrogen gas had been done before any oxidation steps. Therefore, it was determined that changing the atmosphere and/or time heated at 800°C in the current hot cell procedure would not be useful in reducing the sulfur and carbon quantities. The quantities of carbon and sulfur in the Nd material (8 wt % combined) prepared by using the current hot cell process are consistent with the current estimate of sulfur and carbon in the Cm material (about 10 wt % combined). These results seem to confirm the use of that estimate in the current thermal calculations. As stated, sulfur was the dominant contaminant in the Nd material, and XRD found it mostly contained within an Nd<sub>2</sub>O<sub>2</sub>SO<sub>4</sub> compound. Other research suggests that curium forms an oxysulfate compound just as Nd does under similar processing conditions at 900°C [16, 17]. Based on this information, it is most likely that Cm oxysulfate (Cm<sub>2</sub>O<sub>2</sub>SO<sub>4</sub>) is formed along with the oxide during the current process used in the hot cell.

From the data it was seen that at 800°C and 1000°C, the conversion to the oxide was limited as expected since decomposition of Nd oxysulfate to Nd oxide occurs from 1170°C to 1355°C [7, 12]. Therefore, it was found that heating at 1400°C in static air achieved very low sulfur content as well as conversion of the Nd-loaded resin into Nd<sub>2</sub>O<sub>3</sub>. Similar research using Cm [8] prepared the oxide from Cm-loaded resin at 1175°C. These results suggest that to decompose the loaded resin into an oxide and to lower the sulfur content, higher temperatures need to be used; however, flowing air may need to be implemented instead of static air at 1400°C to avoid production of the hydroxide. As mentioned in Section 4.1.3, some of the samples heated to 1400°C revealed that Nd(OH)<sub>3</sub> was present. Although complete conversion of Nd(OH)<sub>3</sub> to Nd<sub>2</sub>O<sub>3</sub> can be performed at ~500°C, previous work has shown that heating Nd oxide at an elevated temperature range up to 200°C for a period of time in an atmosphere containing moisture will lead to hydroxide formation [18]. This could have occurred, depending on the amount of water vapor present in the static atmosphere of the furnace, when it was cooling down during the 1400°C heating procedure. A more controlled atmosphere or a mild quenching could likely avoid this type of formation. Other research also suggests the possibility of forming hydroxides from a reaction at room temperature with moisture

and some rare earth oxides [19]. Based on enthalpies of formation, some precautions might be taken to control the atmosphere when forming Cm oxide [ $\text{Cm}_2\text{O}_3$ ,  $\Delta_f H^\circ_{298\text{ K}} = -1684 \text{ kJ mol}^{-1}$ ] [20], since the possibility of forming the hydroxide [ $\text{Cm}(\text{OH})_3$ ,  $\Delta_f H^\circ_{298\text{ K}} = -1341 \text{ kJ mol}^{-1}$ ] [21] exists if the atmospheric conditions are adequate.

Additional parameters of the product were also considered. The reference hot cell process passes all microsphere particles through a 210  $\mu\text{m}$  screen [1], and those particles passing through are considered to be predominately spherical. The Nd oxide particles analyzed with the SEM showed particle sizes much smaller than the 210  $\mu\text{m}$  limit. Although fragmentation of the microspheres was seen, it has been shown that fragmentation does not occur at higher temperatures with a slower ramp rate [4]. The analysis of the particle characteristics can be important, but it was determined that since all particles under 210  $\mu\text{m}$  are included, no influential recommendations could be given based on size or shape of the particles, especially without more in-depth analysis of the topic. Also, consideration was given to the role that the multiple oxidation states observed in curium would have on its final product. Using cerium as a surrogate might accomplish this goal because it has the same +3 and +4 oxidation states as curium and produces similar oxides [22]. However, further research on the prepared cerium–oxygen system ( $\text{CeO}_x$ ) composition, comparable to that on the complicated curium–oxygen system ( $\text{CmO}_x$ ) [23], would be needed. With the goal of the work presented here to identify the impurity content of the oxide, it was decided that neodymium would be a suitable surrogate for curium.

## 6. SUMMARY

To understand and quantify the carbon and sulfur contents of the curium oxide production process performed in hot cells at the REDC, neodymium was used as a non-radioactive surrogate in a similar oxide formation process. The neodymium was loaded onto a Dowex® resin and treated under various heating conditions. The surrogate product was analyzed for carbon and sulfur impurities. The results indicate that the total amounts of carbon plus sulfur impurities in the Nd product material were very similar to current estimations for curium oxide produced in the hot cell. When using the Cm oxide hot cell processing parameters for preparation of Nd oxide, the majority of the residual sulfur was in the form of a Nd oxysulfate ( $\text{Nd}_2\text{O}_2\text{SO}_4$ ) compound, and it is likely that Cm also forms the homologous oxysulfate compound ( $\text{Cm}_2\text{O}_2\text{SO}_4$ ) under similar heating conditions. Neodymium oxide was formed when the calcination temperature was increased from 1000°C to 1400°C and better removal of carbon and sulfur was observed. This research demonstrated that temperature was the major variable in significantly reducing the carbon and sulfur contaminants from the levels seen in the Nd sample under a replication of the REDC hot cell process to produce Cm oxide.

## REFERENCES

1. F. R. Chattin, E. D. Benker, H. M. Lloyd, B. P. Orr, G. R. Ross, and T. J. Wiggins, "Preparation of curium-amerium oxide microspheres by resin-bead loading," ACS Symposium Series No. 161, *Transplutonium Elements – Production and Recovery*, 1981.
2. T. G. Chapman, *HFIR Target Design Study*, ORNL-TM-1084, Oak Ridge National Laboratory, September 1965.
3. R. W. Hobbs, *Irradiation of Cm, Ni and Dummy Aluminum Target Rods in HFIR Target Island*, USQD-E-HFIR-2001-001, Oak Ridge National Laboratory, pp. 1–38.
4. S. Voit, B. Ilir, and C. Rawn, *Decomposition of Rare Earth Loaded Resin Particles – Fiscal Year 2010*, ORNL/TM-2010/216, Oak Ridge National Laboratory, 2010.
5. H. R. Williams, H. Ning, M. J. Reece, R. M. Ambrosi, N. P. Bannister, and K. Stephenson "Metal matrix composite fuel for space radioisotope energy sources," *J. Nucl. Mater.* **433**(1-3), 116–123 (2013).
6. C. Lopez, X. Deschanel, J. M. Bart, J. M. Boubals, C. Den Auwer, and E. Simoni. "Solubility of actinide surrogates in nuclear glasses." *J. Nucl. Mater.* **312**(Oct), 76–80 (2002).
7. W. H. Hale, Jr., "Thermal decomposition of neodymium-loaded cation exchange resin," *J. Inorg. Nucl. Chem.* **33**(5), 1227–1232 (1971).
8. S. Szenknect, "Kinetics of structural and microstructural changes at the solid/solution interface during dissolution of cerium(IV)–neodymium(III) oxides," *J. Phys. Chem.* **116**, 12027–12037 (2012).
9. L. Claparede, "Influence of crystallization state and microstructure on the chemical durability of cerium-neodymium mixed oxides," *Inorg. Chem.* **50**(18), 9059–9072 (2011).
10. *Using Ion Exchange Resins*, a guide published by Bio-Rad Laboratories, Catalog # 140-9997.
11. K. T. Jacob, R. Akila, and A. K. Shukla, "Oxygen potentials for the oxidation of rare earth oxysulfides to oxysulfates," *J. Solid State Chem.* **69**(1), 109–115 (1987).
12. M. Leskelä and L. Niinistö, "Thermal decomposition of rare earth oxysulfides in air," *J. Thermal Anal.* **18**(2), 307–314 (1980).
13. R. K. Dwivedi and D. A. R. Kay, "Thermodynamics of the oxidation of rare earth oxysulfides at high temperatures," *Metall. Trans. B* **5B**, 523–528 (1984).
14. R. G. Haire and F. A. Fahey, "The oxysulfates and oxysulfides of americium, curium, and berkelium," *J. Inorg. Nucl. Chem.* **89**, 837–841 (1977).
15. G. V. Samsonov and S. V. Radzikovskaya, "The chemistry of rare-earth and actinide sulfides," *Russian Chem. Rev.* **30**, 28–41 (1961).
16. W. Hale and W. C. Mosley, "Preparation of curium oxysulfate and curium oxide by resin calcination," *J. Inorg. Nucl. Chem.* **35**, 165–171 (1973).
17. G. J. Lumetta, M. C. Thompson, R. A. Penneman, and P. G. Eller, "Curium," Chapter 9 in *The Chemistry of the Actinides and Transactinide Elements*, ed. L. R. Morss, N. M. Edelstein, J. Fuger, and J. J. Katz, Springer, 2006, p. 1419.
18. Y. Takai and T. Tsukatani. *Rare Earth Hydroxide and Method for the Preparation Thereof*, US Patent 6,733,882 B2, May 11, 2004.
19. R. J. M. Konings, "Thermochemical and thermophysical properties of curium and its oxides," *J. Nucl. Mater.* **298**, 255–68 (2001).

20. L. R. Morss and C. W. Williams, "Enthalpies of formation of rare earth and actinide(III) hydroxides; their acid-base relationships and estimation of their thermodynamic properties," *Mater. Res. Soc. Symp. Proc.* **257**, 283–288, 1992.
21. L. R. Saksonova, M. A. Bulatov, V. I. Kononenko, and N. V. Lukin, *Russian J. Inorg. Nucl. Chem.* **35**, 1746–1748 (1990).
22. J. A. Poston Jr., R. V. Siriwardane, E. P. Fisher, and A. L. Miltz, "Thermal decomposition of the rare earth sulfates of cerium(III), cerium(IV), lanthanum(III) and samarium(III)," *Appl. Surface Sci.* **214**, 83–102 (2003).
23. T. D. Chikalla and L. Eyring, "The curium–oxygen system," *J. Inorg. Nucl. Chem.* **31**(1), 85–93 (1969).